Journal of Applied Electrochemistry **34**: 345–348, 2004.

Short communication

An X-ray diffraction and transmission electron microscopy study of Pt–Ru fuel cell catalysts before and after operation

C. ROTH*, N. MARTZ and H. FUESS
Institute for Materials Science, Darmstadt University of Technology, Petersenstrasse 23, D-64287 Darmstadt, Germany
*(*author for correspondence, e-mail: c_roth@tu-darmstadt.de)*

Received 24 April 2003; accepted in revised form 5 November 2003

Key words: fuel cells, nanoparticles, post mortem, Pt–Ru, TEM, XRD

1. Introduction

Binary carbon-supported Pt–Ru catalysts and Pt–Ru blacks are most frequently applied in low temperature polymer electrolyte fuel cell (PEMFC) anodes, since they significantly reduce the catalysts sensitivity towards CO poisoning [1–4]. Thus, drastic losses in fuel cell performance associated with the replacement of expensive pure hydrogen by lower cost alternatives like methanol and reformate can be prevented. It is widely accepted that catalyst structure strongly determines the specific catalytic activity and, consequently, a main topic of fuel cell research is the systematic variation and optimization of distinct structural parameters to match the specific needs of PEMFC technology.

Recently, numerous investigations on structural features and their effect on the catalyst performance have been reported [5–9]. However, the influence of particle size, alloy formation and particle agglomeration on the electrocatalytic activity of the catalyst remains unclear. Another drawback of the majority of these studies is that they were mainly carried out *ex situ* under ambient conditions. Some of the techniques used to determine the catalyst nanostructure are not applicable *in situ*, and therefore, the data obtained is incomplete, since significant changes of the structural parameters may occur under fuel cell working conditions [10, 11]. One approach to overcome this problem is the comparison of measurements before and after fuel cell operation. Two different carbon-supported Pt–Ru (1:1) catalysts were synthesized in the aqueous phase and compared to a commercially-available catalyst from E-TEK. Subsequently, X-ray diffraction (XRD) and transmission electron microscopy (TEM) measurements were carried out on the different binary catalysts before and after operation for two weeks in a single cell fuel cell arrangement. The findings are discussed with respect to the average particle size and the particle distribution on the carbon support.

2. Experimental details

2.1. *Catalyst syntheses*

Carbon black (Vulcan XC-72, Cabot Intern.) with a specific surface area (BET) of about 290 $m^2\ g^{-1}$ was used as a support for all catalysts. Two different Pt–Ru (1:1) catalysts, 20 wt % on Vulcan XC-72 were prepared by an impregnation method in aqueous phase [12, 13]. The only difference in the two syntheses was the reducing agent used (formaldehyde for sample I, hydrazine for sample II) and the pH value. The two in-house synthesized catalysts were compared to a commercially-available carbon-supported Pt–Ru (1:1) catalyst, 20 wt % on carbon, purchased from E-TEK inc.

2.2. *Catalyst characterization*

Initially X-ray fluorescence analysis (XRF) was used to verify the correct implementation of the syntheses and to determine the total metal loading of the carbon support. An Xlab 2000 spectrometer (Spectro Analytical Instruments GmbH) was used for all measurements on the catalyst powders. Specific calibration was realized by measuring a series of metal oxides on carbon as oxygen, in contrast to chloride, gives no contribution to spectral noise. The XRF results obtained were in good agreement with the actual stoichiometric quantities employed for the syntheses (Table 1). Data on the sample crystallinity, the average particle sizes and particle size distributions were obtained by XRD and TEM. X-ray powder diffraction measurements were carried out using a STOE STADI-P, with germanium monochromized CuK_α radiation and a position-sensitive detector with 40° aperture in transmission mode. A Jeol TEM 3010 with an acceleration voltage of 300 kV and LaB_6 cathode was applied to obtain high resolution images of the supported catalysts. Samples were prepared by suspending the catalyst powder in alcohol and

Table 1. Results of the XRF analyses for the different catalysts

Sample	Metal loading /wt %	Pt /at %	Ru /at %
Pt–Ru E-TEK	15	51.3	48.7
Sample I	21	54.5	45.5
Sample II	22	60.5	39.5

depositing a drop of the suspension on a standard copper grid covered with carbon. The structural characterization of the commercial Pt–Ru catalyst and the synthesized binary systems by XRD and TEM before operation has already been published [7].

2.3. *Fuel cell operation*

Membrane electrode assemblies (MEA) of an active electrode area of 25 cm^2 and 0.4 mg cm^{-2} noble metal loading per electrode were manufactured according to a slightly-modified spraying method by Wilson and Gottesfeld [14]. Nafion® 117 (DuPont) was applied as proton conducting membrane and in all cases provided with a standard 20 wt % Pt on Vulcan XC-72 catalyst (E-TEK) at the cathode side, while the anode catalyst was varied in our studies. Hydrogen containing 75 ppm and 150 ppm CO, respectively, was humidified at 85 °C and fed into the preheated cell ($T = 75$ °C) under standard pressure. In DMFC mode, a 1 M aqueous methanol solution was evaporated at 130 °C and fed into the cell ($T = 95$ °C) together with a supporting nitrogen gas flow. Pure oxygen was applied as cathode feed in both cases. The cell was operated with pure hydrogen for several days and two E/i curves were recorded per day in order to monitor the cell performance. The fuel cell then ran on H_2/CO mixtures for two days, until finally an aqueous methanol solution was applied as the anode feed. After about two weeks of continuous operation, the fuel was switched off and the anode catalyst removed from the membrane. The catalyst structure after operation was then studied using XRD and TEM, and these post-mortem results compared to the data obtained before operation.

3. Results

The two synthesized catalysts (sample I and II) were characterized by XRD and TEM before and after fuel cell operation and compared to a commercial Pt–Ru catalyst purchased from E-TEK. TEM images of the commercially available catalyst show highly dispersed metallic nanocrystallites on the carbon support grains having an average particle size of about 2 nm. Very similar TEM results were obtained after operation; the particles maintain their high dispersion on the carbon support and only a slight particle growth, up to an average particle size of 4 nm, is found (electron micrographs for the commercial catalyst not shown). In contrast to the commercial catalyst, the nanocrystallites in the synthesized samples tend to form larger agglomerates of about 30 nm. These are either spherical (sample II, Figure 2(a)) or rather irregular in shape (sample I, Figure 1(a)), and are composed of aggregates of individual nanocrystallites of about 5 nm. However, after operation a completely different situation occurs for sample I and II. While the TEM images of sample I still show agglomerates consisting of smaller nanocrystallites (Figure 1(b)), micrographs for sample II display catalytic active metal particles highly dispersed on the support after operation. Consequently, the operation conditions cause the larger nanoparticle aggregates to deagglomerate into individual nanocrystallites during fuel cell operation. Similar results were observed for a ternary Pt–Ru–Mo catalyst, which was also synthesized by an impregnation method in aqueous phase using hydrazine as reducing agent [15].

Evidence for the separation of the agglomerates into individual nanocrystallites has also been observed in the diffraction data (Figure 3(a)–(c)). Despite the different syntheses the powder patterns of all three Pt–Ru

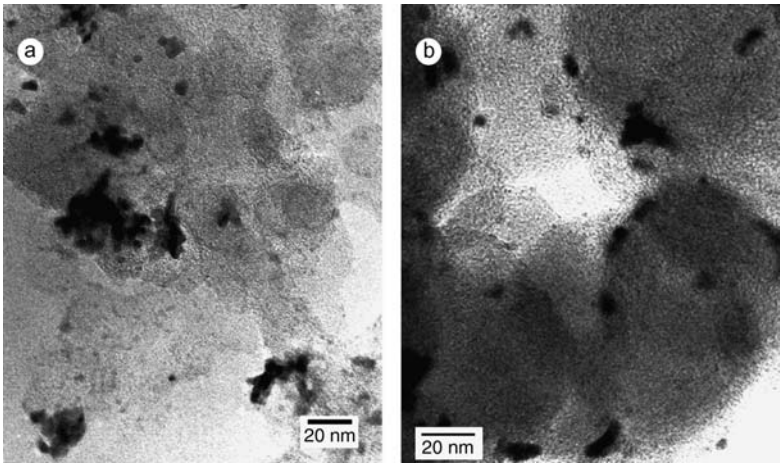

Fig. 1. Typical TEM images of Pt–Ru sample I, before operation (a) compared to the same catalyst after operation (b).

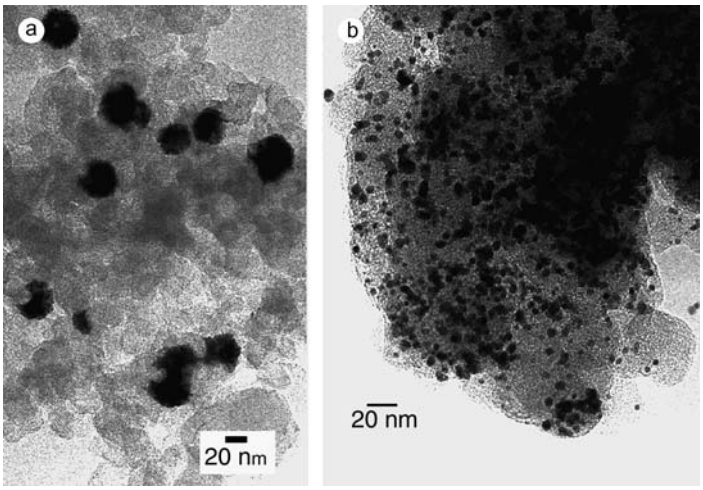

Fig. 2. Comparison of a typical TEM image of Pt–Ru sample II before operation (a) with the same catalyst post-mortem (b).

catalysts in the as-synthesized state look alike, exhibiting the characteristic reflections of the platinum f.c.c. structure. Differences appear only for the reflection width (FWHM), which is an indication for the average particle size and has been evaluated using the Scherrer equation. For the synthesized catalysts, the particle sizes obtained before operation were larger than those of the E-TEK catalyst with average sizes of 7 nm (sample I) and 9 nm (sample II), respectively. These values, however, might be larger than the actual particle size, since the XRD method cannot distinguish between individual nanocrystals if they have similar orientation within a larger aggregate [16].

For the commercially-available Pt–Ru system and sample I a slight particle growth is observed after operation for two weeks in a fuel cell (Table 2). The average sizes increase from 2 to 4 nm (E-TEK) and from 7 to 8 nm for sample I (Figure 3(a) and (b)). For sample

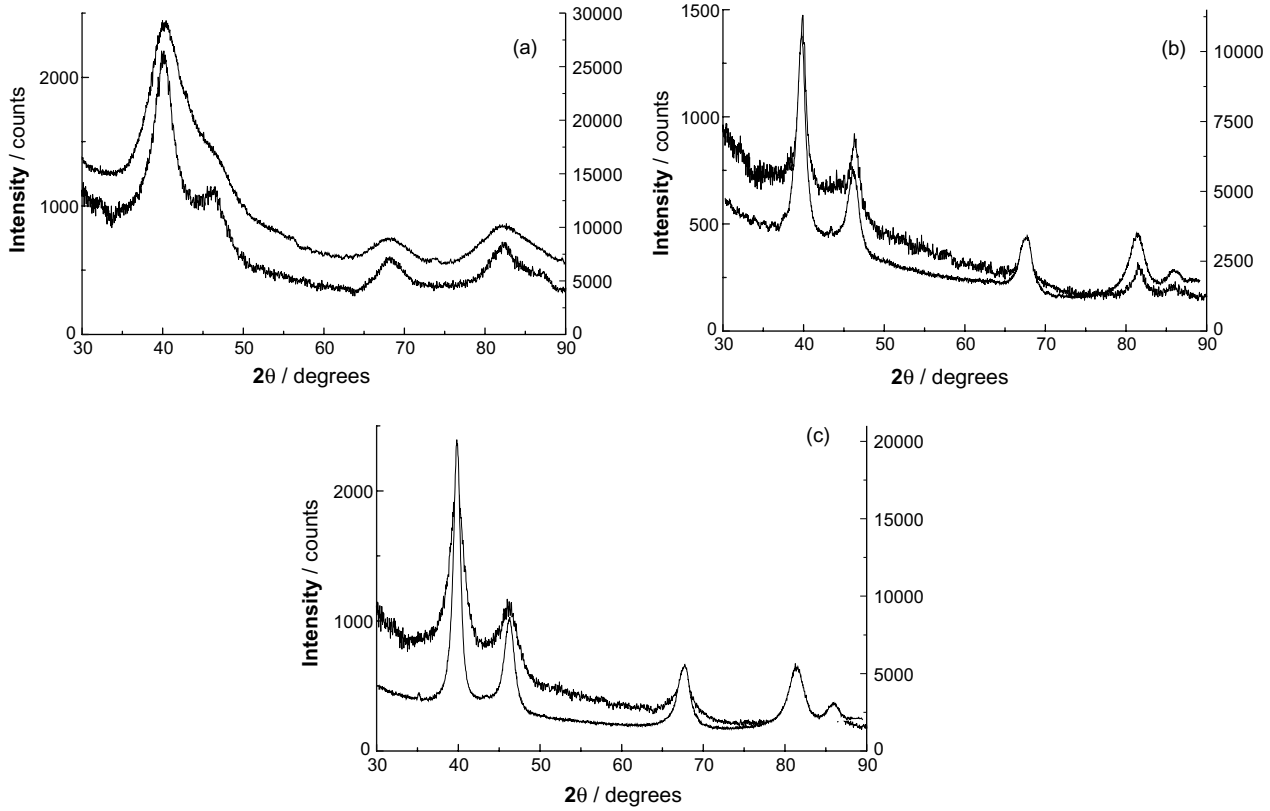

Fig. 3. Comparison of the X-ray patterns of the different samples before (light grey) and after operation (black); (a) commercial catalyst, (b) sample I and (c) sample II.

Table 2. Comparison of the particle sizes determined by XRD before and after operation

Sample	Particle size before operation /nm	Particle size after operation /nm
Pt–Ru E-TEK	2	4
Pt–Ru sample I	7	8
Pt–Ru sample II	9	5

II, however, the opposite is found after operation; the post-mortem X-ray pattern reveals a smaller average size than before operation. The particle size decreases from 9 to 5 nm, and this can only be understood from the TEM results. Before operation, the nanocrystallites are situated within an agglomerate and particles with similar orientations are counted and measured as one bigger particle with higher microstrain. Consequently, the resulting average particle size is slightly higher than the actual one. After operation, these larger aggregates deagglomerate into their individual nanocrystalline components, and the average size determined is the size of distinct and separate particles with apparently less microstrain. Thus, the diffraction and the TEM data are in excellent agreement and lead to the same conclusions. Further investigations of the reason and the mechanism for the separation of larger agglomerates under working conditions are required to understand this effect and use it for the development of future catalyst preparation routes. However, the results show that catalysts which do not look promising before operation because of large average particle sizes and pronounced particle agglomeration may develop into successful systems after they have been subjected to fuel cell working conditions.

4. Conclusion

The present work demonstrates changes in the nanomorphology of different Pt–Ru catalysts after two weeks' operation in a PEM fuel cell using hydrogen, hydrogen/CO mixtures and methanol as the anode feed. Two catalysts were synthesized and then investigated by XRD and TEM before and after operation, and the results compared to a commercially-available Pt–Ru system. But while the commercial catalyst and sample I undergo only minor changes during operation, sample II displays significant structural changes. XRD and TEM data show that the as-synthesized catalyst consists of large particle aggregates approximately 30 nm in size. However, these separate into individual and highly-dispersed nanocrystallites during fuel cell operation.

The results indicate that catalysts which look comparatively poor before operation consisting of large particles with a high degree of agglomeration may develop into promising catalysts when subjected to operating conditions. Consequently, the catalyst structure needs to be analysed after operation, otherwise auspicious catalysts may be rejected only because of their poor appearance. However, additional investigations as to why and how larger agglomerates can separate into individual nanocrystallites under operating conditions and how this improves the catalyst activity are required.

In this context, the weak point of the investigations presented is that the catalysts were operated for two weeks in different modes using hydrogen, H_2/CO and methanol as the anode feed. Thus, it is not possible to distinguish between the influence of the change in potential, temperature and anode feed, respectively. For a more comprehensive study, the catalyst should be characterized after certain stages during operation in hydrogen, in H_2/CO and after operation in methanol. At the same time, current–voltage curves have to be recorded to monitor the catalyst activity at each stage. However, the most elegant solution would obviously be to follow changes in the catalyst structure *in situ* using XRD and X-ray absorption spectroscopy.

Acknowledgement

Financial support of the Deutsche Forschungsgemeinschaft and the Fonds der Chemischen Industrie is gratefully acknowledged.

References

1. H.A. Gasteiger, N.M. Markovic, P.N. Ross and E.J. Cairns, *J. Phys. Chem.* **97** (1993) 12020.
2. H.A. Gasteiger, N.M. Markovic, P.N. Ross and E.J. Cairns, *J. Phys. Chem.* **98** (1994) 617.
3. J. Divisek, H.-F. Oetjen, V. Peinecke, V.M. Schmidt and U. Stimming, *Electrochim. Acta* **43** (1998) 3811.
4. C. Roth, N. Martz, F. Hahn, J.-M. Leger, C. Lamy and H. Fuess, *J. Electrochem. Soc.* **149** (2002) E433.
5. A.S. Arico, P. Creti, H. Kim, R. Mantegna, N. Giordano and V. Antonucci, *J. Electrochem. Soc.* **143** (1996) 3950.
6. D.R. Rolinson, P.L. Hagans, K.E. Swider and J.W. Long, *Langmuir* **15** (1999) 774.
7. C. Roth, N. Martz and H. Fuess, *Phys. Chem. Chem. Phys.* **3** (2001) 315.
8. C.W. Hills, M.S. Nashner, A.I. Frenkel, J.R. Shapley and R.G. Nuzzo, *Langmuir* **15** (1999) 690.
9. T. Iwasita, H. Hoster, A. John-Anacker, W.F. Lin and W. Vielstich, *Langmuir* **16** (2000) 522.
10. W.E. O'Grady, P.L. Hagans, K.I. Pandya and D.L. Maricle, *Langmuir* **17** (2001) 3047.
11. R. Viswanathan, G. Hou, R. Liu, S.R. Bare, F. Modica, G. Mickelson, C.U. Segre, N. Leyarovska and E.S. Smotkin, *J. Phys. Chem. B* **106** (2002) 3458.
12. E. Auer, A. Freund, T. Lehmann, K.-A. Starz, R. Schwarz and U. Stenke, EP 0 880 188 A2.
13. J.B. Goodenough, A. Hamnett, B.J. Kennedy, R. Manoharan and S.A. Weeks, *Electrochim. Acta* **35** (1990) 199.
14. M.S. Wilson and S. Gottesfeld, *J. Appl. Electrochem.* **22** (1992) 1.
15. N. Martz, C. Roth and H. Fuess, in preparation.
16. D. Rafaja, private communication (March 2003).